Extraction and Characterization of Microcrystalline Cellulose Derived from Kapok Fibre (*Ceiba pentandra*) via Facile Chemical Alkali Treatment

Mohamad Fakhrul Hisham Hashim[1], Zul Adlan Mohd Hir[1,2,*], Shaari Daud[1], Hartini Ahmad Rafaie[3] and Mohamad Azuwa Mohamed[4]

[1]Faculty of Applied Sciences, Universiti Teknologi MARA Pahang, 26400 Bandar Tun Abdul Razak Jengka, Pahang, Malaysia

[2]Catalysis for Sustainable Water and Energy Nexus Research Group, School of Chemical Engineering, College of Engineering, Universiti Teknologi MARA, 40450 Shah Alam, Selangor, Malaysia

[3]Centre of Foundation Studies, Universiti Teknologi MARA, Selangor Branch, Dengkil Campus, 43800 Dengkil, Selangor, Malaysia

[4]Department of Chemical Sciences, Faculty of Science and Technology, Universiti Kebangsaan Malaysia, 43600 UKM Bangi, Selangor, Malaysia

*Corresponding author (e-mail: zuladlan@uitm.edu.my)

Due to its excellent qualities, microcrystalline cellulose (MCC) has been used in several applications including polymer composites, packaging materials, and medicinal compounds. However, the insufficiency of non-renewable resources has turned the attention of researchers to greener strategies for raw materials derived from renewable sources. This work aimed to extract microcrystalline cellulose (MCC) from kapok fibre (*Ceiba pentandra*) by means of chemical alkali treatment using 5 % (w/v) NaOH, and acidified bleaching treatment with 2 % (w/v) NaClO. The obtained MCC was characterized for its morphology, structural and thermal stability, and crystallinity, through scanning electron microscopy coupled with energy dispersive X-ray (SEM-EDX), Fourier Transform infrared spectroscopy (FTIR), thermogravimetric (TGA) and X-ray diffraction (XRD) analyses. Kapok fibre exhibited rod-like shapes with a smooth surface and a diameter of about 7.25 µm. This was transformed into a rough surface and whiter colour after going through the process of chemical treatment, in which the fibre diameter also decreased to 3.04 µm. The TGA curves for both kapok and MCC indicated weight loss at 236 °C to 355 °C for the first decomposition stage due to the thermal degradation of cellulose and hemicellulose, then further thermal decomposition until 900 °C. XRD analysis indicated no significant differences in crystallite size (0.04 - 1.70 nm) and crystallinity index values (20.6 - 46.0 %). In conclusion, the cost-effective MCC derived from kapok fibre is a promising renewable and sustainable resource which has potential for extensive utilization across many industrial applications.

Keywords: Kapok fibre; *Ceiba pentandra*; extraction; plant fibre; microcrystalline cellulose

Received: February 2024; Accepted: May 2024

In recent times, there has been a concerning trend of excessive exploitation of non-renewable resources. This unrestricted usage not only has a negative impact on environmental sustainability, but also poses a significant threat to public health. Numerous researchers have been drawn to the use of raw materials from renewable sources because of the scarcity of non-renewable resources. This is also because of the desire for renewable sources, and the need for methods that are in compliance with environmental regulations [1]. Considering this dilemma, cellulose is regarded as one of the earth's most abundant and best renewable natural biopolymers that can be extracted from plant biomass [2, 3]. Cellulose is the polymeric unit of glucose with the chemical formula $(C_6H_{10}O_5)_n$ and is made up of several repeating units of polysaccharide β-D-glucopyranose linked by β-1-4-glycosidic bonds. It is possible to modify cellulose to create a variety of useful derivative products such as nanocrystalline cellulose (NCC) and microcrystalline cellulose (MCC) for water treatment, agriculture, pharmaceutical and many more applications [4-6].

MCC is an odourless, tasteless crystalline powder that can be produced by hydrolysing cellulose in an acidic medium. It is the pure product of cellulose depolymerization obtained by acid hydrolysis of native cellulose [7]. In addition, due to its fine particle size, large surface area, renewability, mechanical strength and water insolubility, it has great potential in the pharmaceutical and food sectors (as packaging materials, stabilizers, antimicrobial agents), agriculture and textile industry (as emerging adsorbents for the removal of dyes and heavy metals) and also the

medical sector (as an entrapment material) [8-11]. According to the literature, numerous sources are used in the manufacturing of MCC, such as kapok fibre [12-14], coconut husk fibre [4], hardwood pulp [15], seaweed [5], walnut, almond and apricot stone shells [7] and corncobs [16].

In the context of Malaysia, kapok, sometimes referred as 'kekabu' in the local vernacular, has traditionally been used as a cushioning material for pillows and beds. Basically, it is pale yellowish-brown in colour, light-weight, fluffy and significantly hydrophobic [17]. Its structure possesses a hollow composition and consists of cellulosic fibres containing cellulose, hemicellulose, lignin, pectin and having a waxy surface [18]. This distinguishes kapok fibre (KF) from other natural fibres due to its porosity, which is greater than 80 % [19]. Due to its waxy surface, KF is ineffective against hydrophilic agents/ substances. Nevertheless, this limitation can be mitigated with the implementation of surface modification techniques such as chemical and oxidation treatments [20]. For example, chemical processing involving the use of alkali and acid can effectively remove the lignin, pectin, natural oils and wax present on the external surface of the fibre. The phenolic chemicals that can transform it from hydrophobic to hydrophilic are then eliminated by oxidation processes [12]. KF is a low-cost material that is now being used in place of other types of plant biomass because of its capacity for rapid growth, high quantity of cellulose, and excellent mechanical properties [21]. In addition to improving kapok fibre versatility for usage in industrial applications, the manufacturing of MCC from kapok fibre would have a positive impact on the regional economy.

Thus, in this work, we investigated the extraction of MCC from KF (*Ceiba pentandra*) by means of a simple and inexpensive method. The extraction process involved chemical alkali ($NaOH/NaClO_2$), and acidified bleaching (HNO_3) treatments. Morphological and structural analyses were carried out using scanning electron microscopy equipped with energy dispersive X-ray (SEM-EDX), Fourier Transform infrared (FTIR) spectroscopy, thermogravimetric analysis (TGA-DTG), and X-ray diffraction (XRD). In addition to being renewable, economical, accessible, reasonably easy to extract, biocompatible and non-toxic, this method is also a potential alternate approach to address the problems of environmental contamination with a broad range of industrial applications. Abdullah et al. (2024) employed MCC sourced from KF to investigate water flux and methylene blue rejection. The results demonstrated a remarkable rejection rate of up to 90 % [22]. Similarly, Futalan et al. (2022) modified KF using the same methodology and implemented it for the adsorption of dyes and heavy metal ions from aqueous solutions [12]. As MCC surfaces feature numerous -OH groups, they encourage surface modification that can expand their industrial application without any negative effects. The motivation for this work is implied by the aforementioned benefits of employing these fibres for microcellulose extraction, particularly their high cellulose content and increasing market demand.

EXPERIMENTAL

Chemicals and Materials

The kapok fibre (*Ceiba pentandra*) used in this study was sourced from Taman Tasik Permaisuri, Cheras, Kuala Lumpur. The fibre was separated from the seeds and fruit husk. The raw fibre underwent a process in which any visible dust and particles were removed. Sodium hydroxide (NaOH) pellets, nitric acid (HNO_3, 65 %), and sodium chlorite ($NaClO_2$, 80 %) were purchased from R&M Chemicals (Malaysia) and used as received. Deionized water was used throughout the experimental procedure [19, 21].

Extraction of MCC from Kapok Fibre

The process of cellulose extraction was initiated by subjecting the kapok fibre (*Ceiba pentandra*) sample to alkali treatment using NaOH solution, as presented in Figure 1. In this experiment, 20 g kapok fibre was added to 800 mL of 5 % (w/v) sodium hydroxide (NaOH) solution, then boiled at 125 °C for 2 hours with constant stirring. After that, the sample was rinsed repeatedly with distilled water until it achieved a neutral pH. Subsequently, the extraction process was followed by the conventional acidified bleaching technique involving $NaClO_2$ treatment. The sample was subjected to a second boiling process using 800 mL of 2 % (w/v) $NaClO_2$ solution at 125 °C for 2 hours. A small volume of 60 % (v/v) HNO_3 was introduced into the mixture. A white sample was obtained after two iterations of the $NaClO_2$ treatment.

Characterization Methods

Surface morphological elemental composition analysis and mapping of KF and MCC were performed using scanning electron microscopy equipped with an energy dispersive X-ray analyzer (SEM-EDX, TESCAN VEGA 3) at 400x and 1000x magnification. The fibre diameter was measured by ImageJ software. The functional groups of KF and MCC were analysed by Fourier Transform infrared spectroscopy (FTIR) within the 500 to 4000 cm^{-1} range on a Perkin Elmer Spectrum 400 (FT-IR/FT-NIR) spectrometer. The thermal stability of both KF and MCC were characterized by employing thermogravimetric analysis (TGA, NETZSCH TG). The analysis was conducted in a nitrogen environment with a heating rate of 10 °C min^{-1} over a temperature range of 100 - 1000 °C.

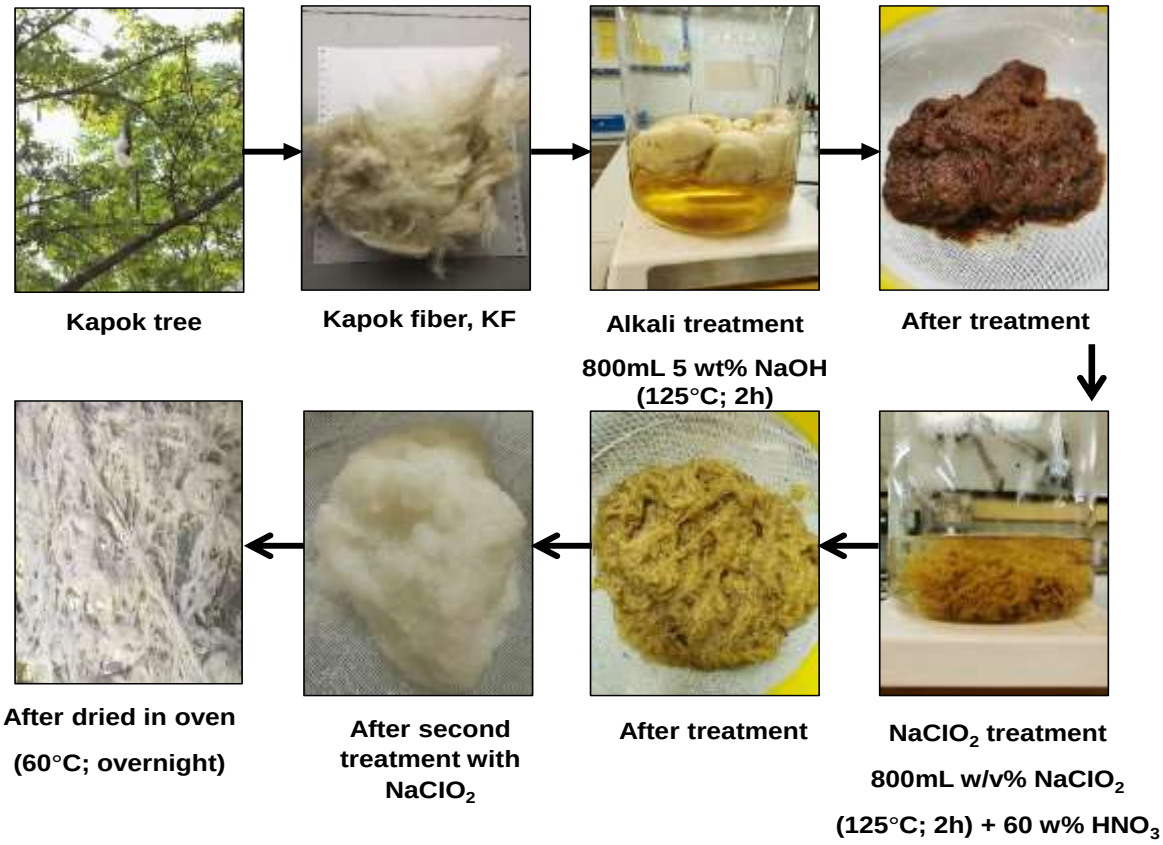

Figure 1. Overview of MCC experimental procedure.

The X-ray diffraction (XRD) patterns of KF and MCC were acquired using a PANalytical X'pert PRO, employing Cu-Kα radiation with λ=0.15418 nm. The scanning rate was set at 0.05° 2θ s^{-1}. Average particle sizes were calculated using the Debye-Scherrer equation, Eq. (1):

$$D = \frac{K\lambda}{\beta \cos\theta} \quad (1)$$

In the given context, D represents the particle size, K denotes Scherrer's constant (K=0.94), λ is the X-ray wavelength (0.15418 nm), β represents the full width at half maximum (FWHM) of the diffraction peak and θ indicates the angle of diffraction.

The determination of crystallinity in the samples was conducted by analysing diffraction intensity data through the utilization of an empirical approach specifically designed for native cellulose. The material's crystalline to amorphous ratio was determined by Segal's equation, Eq. (2):

$$\text{Cr.I}\,(\%) = \frac{I_{200} - I_{am}}{I_{200}}\, x\, 100 \quad (2)$$

where Cr.I is the crystallinity index, I_{200} represents the highest intensity of the diffraction from the 200 plane recorded at 2θ = 22.6° and I_{am} denotes the lowest intensity observed at 2θ = 18° (S23 egal Creely, Martin & Conrad, 1959) [24].

RESULTS AND DISCUSSION

Figure 2 shows the morphological characteristics of KF and MCC that were seen at 400x and 1000x magnification. It can be observed that KF had a smooth surface and rod-like shape with a diameter of 7.25 µm. Chemical treatments caused the surface structure to break down and degrade, causing the fibre morphology to become tangled, which led to the production of MCC with a diameter of 3.04 µm. The lower amounts of lignin and hemicellulose also resulted in the fibre's rough surface and colour change, as well as the reduced fibre diameter.

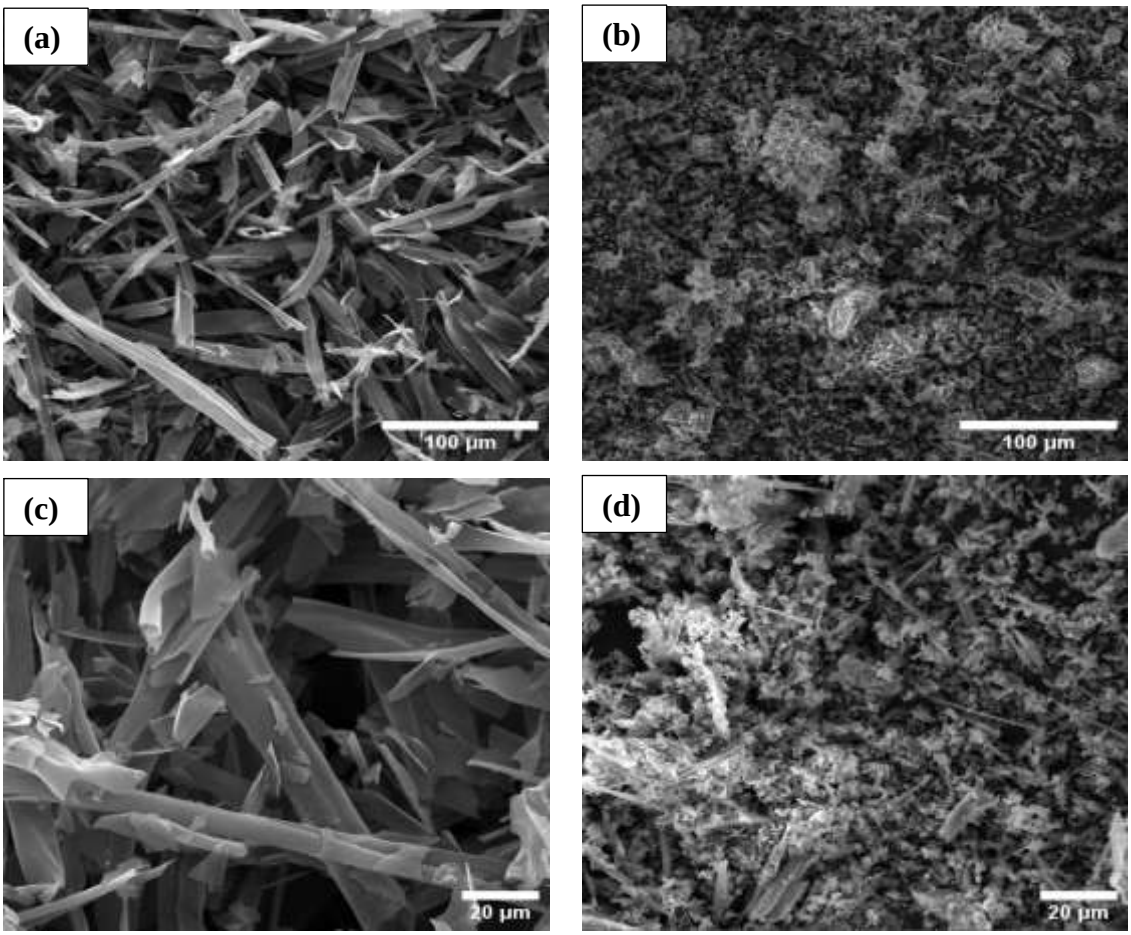

Figure 2. SEM images of (a) KF; 400x (b) MCC; 400x, (c) KF; 1Kx (d) MCC; 1Kx.

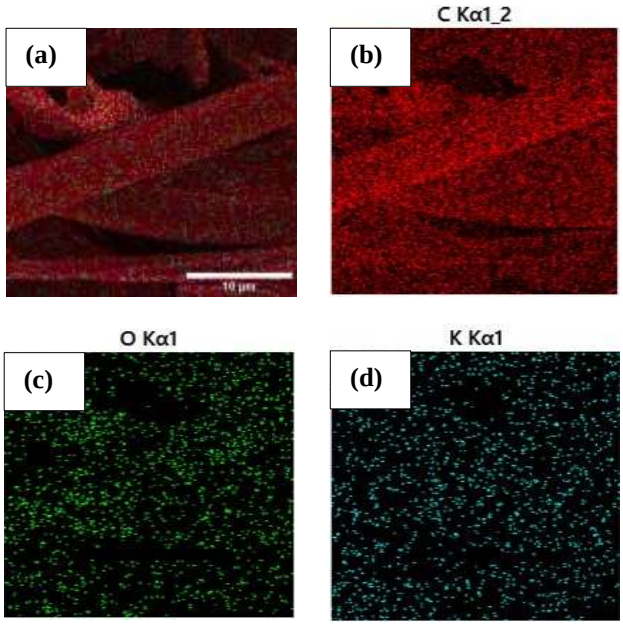

Figure 3. EDX analysis image of KF (a) and the related C, O and K elemental mapping images are displayed in (b), (c) and (d) respectively.

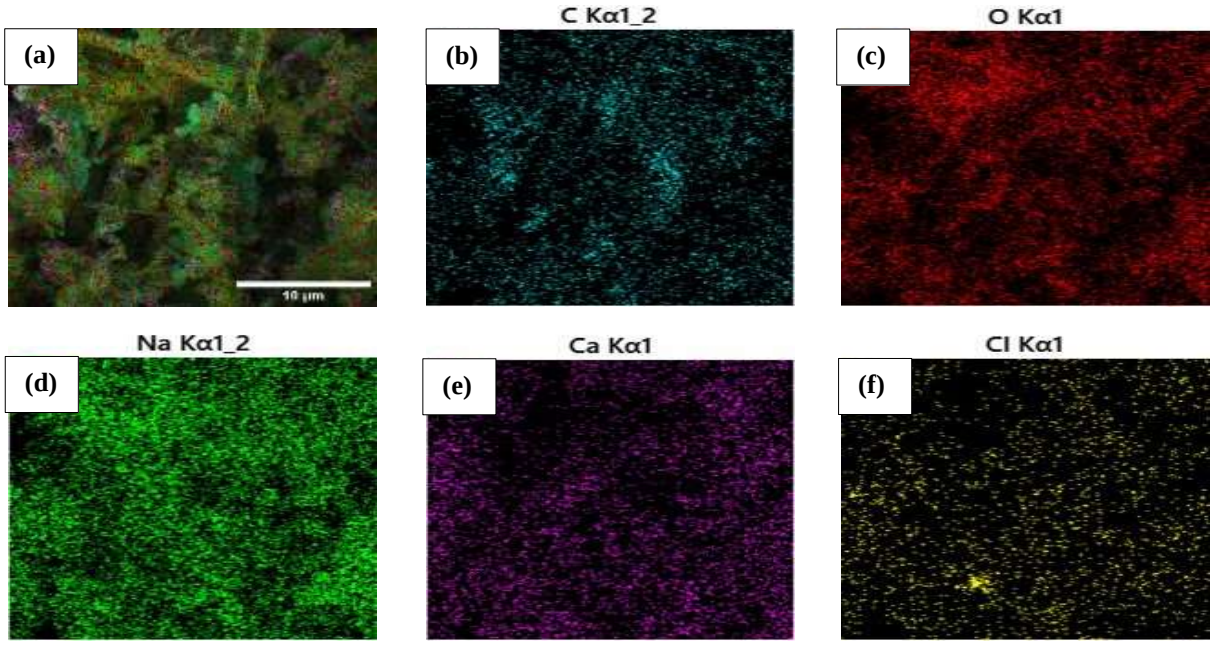

Figure 4. EDX analysis image of MCC (a) and the related C, O, Na, Ca and Cl elemental mapping images are displayed in (b), (c), (d), (e) and (f) respectively.

The energy dispersive X-ray spectroscopy (EDX) and chemical mapping analysis results are presented in Figures 3 and 4, respectively, along with the elemental composition. Figure 5 shows the distinctive peaks of KF and MCC. The primary elements in KF were carbon (C) and oxygen (O), confirming the purity of the sample. The EDX analysis revealed the presence of sodium (Na), chlorine (Cl) and calcium (Ca) after the treatment. Elements are represented by red and green for C and O in KF, and red, green, blue, and yellow for O, Na, C, and Cl respectively in MCC

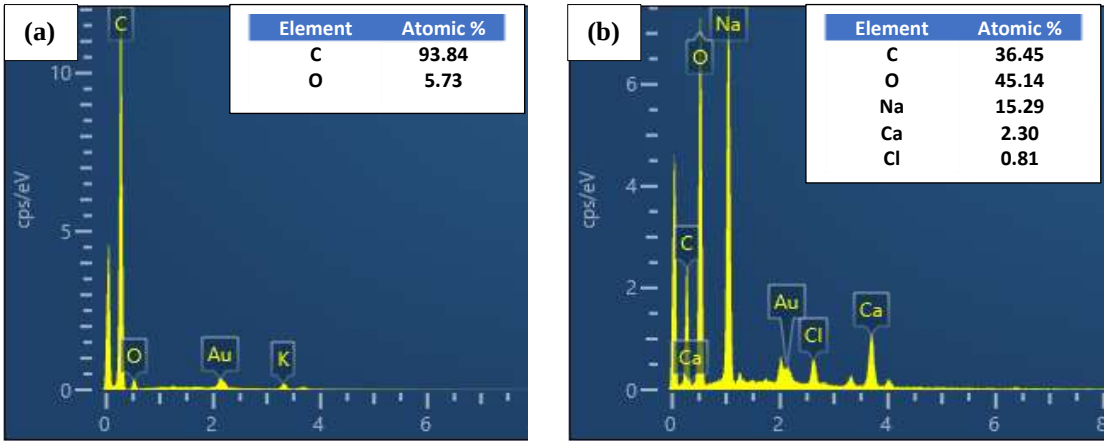

Figure 5. EDX spectrum and composition of (a) KF, and (b) MCC.

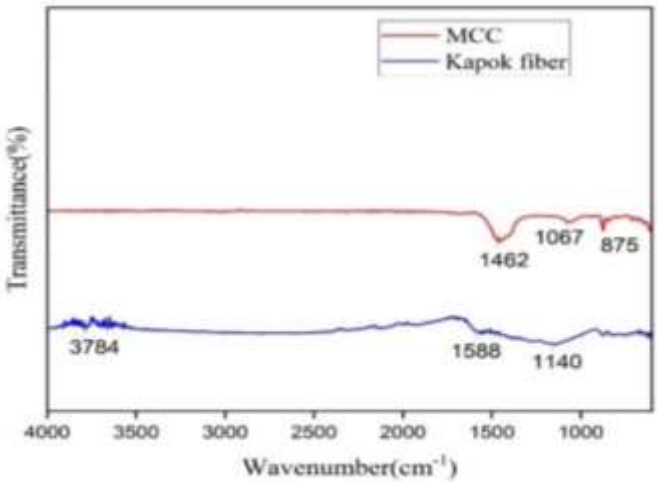

Figure 6. FTIR spectra of KF and MCC.

FTIR analysis was conducted to examine alterations in composition, structure and functional groups during each phase of MCC isolation. The removal of cellulose and lignin in the fibre by treatment has the potential to enhance the surface topography, solubility and reactivity of KF. The alkaline treatment method employed the use of a robust base, such as NaOH and $NaClO_2$, to effectively eliminate wax, lignin and other contaminants. Figure 6 displays the spectra of KF and MCC.

Generally, the absorption bands show several similar functional groups. Nevertheless, there were changes in the intensity of the absorption bands at 1462 cm^{-1}, 1067 cm^{-1} and 875 cm^{-1} .The spectra of KF showed a band between 3600 to 3800 cm^{-1}, which is indicative of O-H stretching in cellulose, hemicellulose and lignin [12]. The peak of the O-H group was in the range stated by Vasu et al. (2021), which was 4000–2995 cm^{-1} [6]. Lignin was present at 1500–1600 cm^{-1} corresponding to the aromatic skeletal vibration. The presence of C=C unsaturated linkages, notably aromatic rings within the lignin, was confirmed by the absorption band at 1588 cm^{-1} in KF. Sodium chlorite was used to eliminate the waxy material on the surface of the kapok fibres. The increase in the intensity of the band at 1462 cm^{-1} in MCC was associated with the presence of the carbonyl group (C=O) and potential for wax removal from the kapok fibre surface.

The TGA results are presented in Figure 7, and illustrates the relationship between weight percentage (%) and temperature (°C). The curve demonstrates that both samples initiated a degradation process at approximately the same time. There were two main weight loss processes for kapok fibre and MCC, starting with a weight loss of about 3 % in range of 100 °C to 236.7 °C. At this stage, the weight loss was attributed to the evaporation of moisture or any other volatile compounds within the samples [20]. The first sharp loss was about 60 % from 237 °C to 374 °C, due to the elimination of lignin and corresponding to the thermal degradation of hemicellulose. The second stage of weight loss of 23 % and 30 % was observed for the raw and treated fibres, respectively.

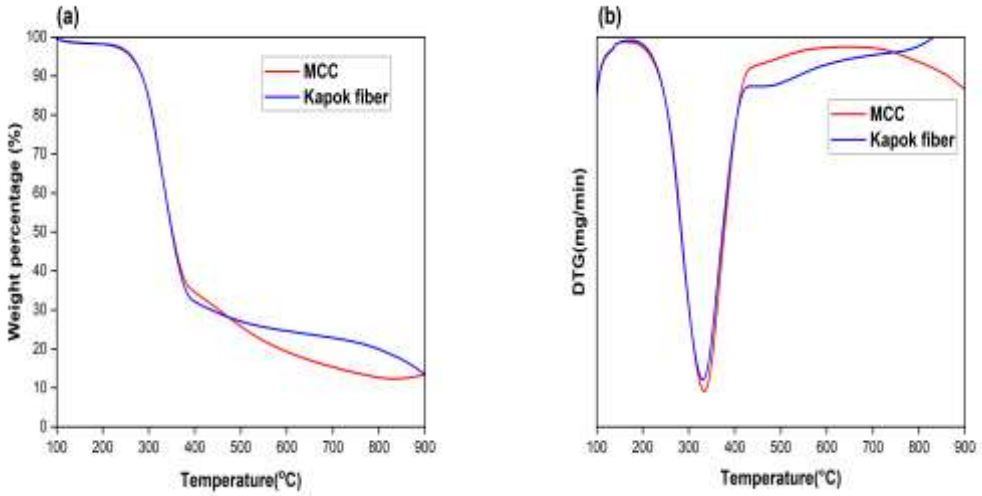

Figure 7. (a)TGA curves, and (b) DTG curves for the kapok fibre and MCC samples.

Table 1. Comparison of activation energy.

Sample	Mass change (%)	Residual mass (%)	Activation energy, Ea, (J/K)
Kapok fibre	87.24	12.76	21.65
MCC	82.38	17.62	22.0

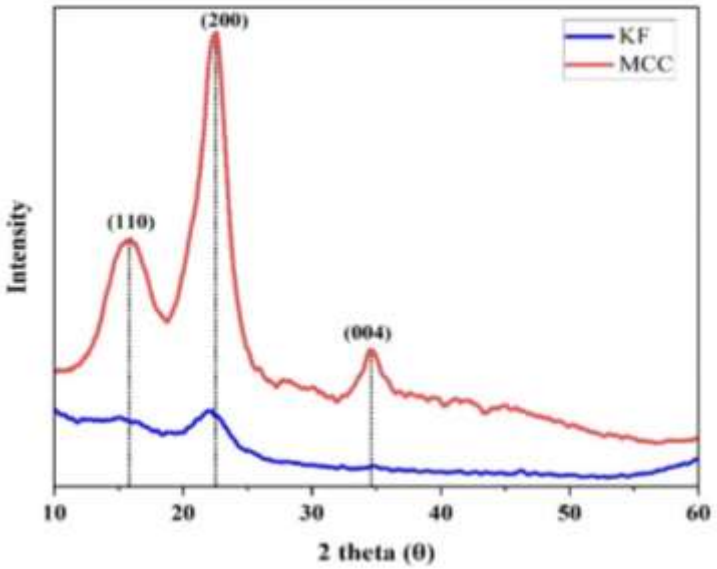

Figure 8. XRD diffraction patterns of KF and MCC

The DTG analysis results obtained for the kapok fibre and MCC indicated thermal stability at the same temperature (334.5 °C) but a slight difference in DTG levels. The TGA and DTG curves of both samples are shown in Figure 6(a) and (b). The weight loss trends for kapok fibre and MCC were similar but showed differences after 400 °C until end of analysis. Table 1 shows the thermal stability of kapok fibre and MCC obtained by calculating the activation energies. The larger the activation energy, the greater the stability.

Figure 8 illustrates the peak patterns observed for KF and MCC which presented at 15.8°, 22.5° and 34.6° corresponding to the (110), (200) and (004) crystal planes, showing the characteristics of the cellulose structure [18,19,23]. The intensity of the peaks observed in MCC was slightly higher in comparison to KF, suggesting a greater degree of compactness and order in the crystalline structure. The crystallite dimension exhibited an increase from 0.043 to 1.71 nm subsequent to the alkali and acid treatment of KF, as shown in Table 2.

The crystallite size increased in parallel with the crystallinity degree, as the initial kapok fibre had a crystallinity of 20.6 %, which then increased to 46.0 %. The observed increase can be attributed to the degradation of the amorphous component of lignin, hemicellulose and kapok fibre, as well as an increase in the degree of crystallinity [26]. This is consistent with a previous study that showed that the increase in crystallinity degree corresponds to an increase in crystallite size [25].

Table 2. Comparison of crystallite size of kapok fibre and MCC.

Material	Crystallite size (nm)			Average	CI (%)
	(110)	(200)	(004)		
Kapok fibre	0.033	0.055	-	0.043	20.6
MCC	0.55	3.55	1.01	1.71	46.0

CONCLUSION

This paper details the successful extraction of cellulose from kapok fibre *(Ceiba pentandra)*. The extraction involved alkali and acid treatment, using 5 % (w/v) NaOH as well as $NaClO_2$ for bleaching. The successful removal of amorphous cellulose from kapok fibre was achieved through the utilization of a 60 % (v/v) HNO_3 solution. SEM-EDX, FTIR, TGA and XRD results demonstrated that lignin and hemicellulose had been removed. Alkali and acid treatments produced MCC with a rough surface and decreased the fibre dimension from 7.25 µm to 3.04 µm. The crystallite size and crystallinity of the MCC was 1.71 nm and 46.0 %, respectively, which were higher than that of kapok fibre.

ACKNOWLEDGEMENTS

The authors gratefully acknowledge Universiti Teknologi MARA (UiTM) Pahang Branch through the GT2P Grant (Project Number: 600-TNCPI 5/3/DDN (06) (014/2023)) and UiTM for Lestari SDG Triangle Grant (600-RMC/LESTARI SDG-T 5/3 (019/ 2021)), as well as the services and facilities provided by Universiti Teknologi MARA (UiTM) Pahang Branch and UiTM Shah Alam to carry out the laboratory work.

REFERENCES

1. Abdul Rahman (Wahida), W., Syafiqah Ismail (Aina), A. & Aishatun Majid (Aishatun), N. (2022) Preparation and characterization of biocomposite film derived from microcrystalline cellulose (MCC) of jackfruit rind waste. *Materials Today: Proceedings*, **66**, 4055–4060.

2. Bahari, S. A., Grigsby, W. J. & Krause, A. (2017) Flexural Properties of PVC/Bamboo Composites under Static and Dynamic-Thermal Conditions: Effects of Composition and Water Absorption. *International Journal of Polymer Science*, **2017**.

3. Ahmad Rafaie, H., Mohd Yusop, N. F., Azmi, N. F., Abdullah, N. S. & Ramli, N. I. T. (2021) Photocatalytic degradation of methylene blue dye solution using different amount of ZnO as a photocatalyst. *Science Letters*, **15**, 1.

4. Abdullah, N. A., Sainorudin, M. H., Rani, M. S. A., Mohammad, M., Kadir, N. H. A. & Asim, N. (2021) Structure and thermal properties of microcrystalline cellulose extracted from coconut husk fiber. *Polimery/Polymers*, **66**, 187–192.

5. Baghel, R. S., Reddy, C. R. K. & Singh, R. P. (2021) Seaweed-based cellulose: Applications, and future perspectives. *Carbohydrate Polymers*, **267**, 118241.

6. Vasu, S., Abu Bakar, A. H., Teh, K. C. & Leng Chew, I. M. (2021) Extraction of nanocrystalline cellulose from Kapok fiber as potential water-resistant composite. *IOP Conference Series: Earth and Environmental Science*, **765**, 012090.

7. Nazir, S., Habib, U. & Ul Islam, T. (2023) Extraction and Characterization of Micro-crystalline Cellulose from Walnut, Almond and Apricot Stone Shells. *Journal of the Chemical Society of Pakistan*, **45**, 85–92.

8. Cheng, J., Wang, H., Xiao, F., Xia, L., Li, L. & Jiang, S. (2021) Functional effectiveness of double essential oils@yam starch/microcrystalline cellulose as active antibacterial packaging. *International Journal of Biological Macromolecules*, **186**, 873–885.

9. Garba, Z. N., Lawan, I., Zhou, W., Zhang, M., Wang, L. & Yuan, Z. (2020) Microcrystalline cellulose (MCC) based materials as emerging adsorbents for the removal of dyes and heavy metals – A review. *Science of the Total Environment*, **717**, 135070.

10. Bangar, S. P., Esua, O. J., Nickhil, C. & Whiteside, W. S. (2023) Microcrystalline cellulose for active food packaging applications: A review. *Food Packaging and Shelf Life*, **36**, 101048.

11. Haldar, D. & Purkait, M. K. (2020) Micro and nanocrystalline cellulose derivatives of ligno-cellulosic biomass: A review on synthesis, applications and advancements. *Carbohydrate Polymers*, **250**, 116937.

12. Futalan, C. M., Choi, A. E. S., Soriano, H. G. O., Cabacungan, M. K. B. & Millare, J. C. (2022) Modification Strategies of Kapok Fiber Composites and Its Application in the Adsorption of Heavy Metal Ions and Dyes from Aqueous Solutions: A Systematic Review. *International Journal of Environmental Research and Public Health*, **19**.

13. Zhang, H., Zhao, T., Chen, Y., Hu, X., Xu, Y., Xu, G., Wang, F., Wang, J. & Shen, H. (2022) A sustainable nanocellulose-based superabsorbent from kapok fiber with advanced oil absorption and recyclability. *Carbohydrate Polymers*, **278**.

14. Gea, S., Andriayani, Piliang, A. F. R., Attaurrazaq, B., Rahayu, S. & Hendrana, S. (2023) Evaluation to possibility of cellulose fibers isolated from kapok randu (Ceiba Pentandra) as a precursor growth of carbon micro structures with the assist of metal catalysts. *Journal of King Saud University - Science*, **35**, 102423.

15. Yavorov, N., Valchev, I., Radeva, G. & Todorova, D. (2020) Kinetic investigation of dilute acid

hydrolysis of hardwood pulp for microcrystalline cellulose production. *Carbohydrate Research*, **488**, 107910.

16. Shao, X., Wang, J., Liu, Z., Hu, N., Liu, M. & Xu, Y. (2020) Preparation and Characterization of Porous Microcrystalline Cellulose from Corncob. *Industrial Crops and Products*, **151**, 1–6.

17. Ye, C. Q. (2012) Sol-gel processes of functional powders and films. *Intech*, **13**.

18. Sangalang, R. H. (2021) Kapok Fiber- Structure, Characteristics and Applications: A Review. *Oriental Journal of Chemistry*, **37(3)**, 513–523.

19. Purnawati, R., Febrianto, F., Wistara, I. N. J., Nikmatin, S., Hidayat, W., Lee, S. H. & Kim, N. H. (2018) Physical and chemical properties of kapok (Ceiba pentandra) and balsa (ochroma pyramidale) fibers. *Journal of the Korean Wood Science and Technology*, **46(4)**, 393–401.

20. Mohamed, M. A., Salleh, W. N. W., Jaafar, J., Ismail, A. F., Abd Mutalib, M., Mohamad, A. B., Zain, M. F., Awang, N. A. & Mohd Hir, Z. A. (2017) Physicochemical characterization of cellulose nanocrystal and nanoporous self-assembled CNC membrane derived from Ceiba pentandra. *Carbohydrate Polymers*, **157**, 1892–1902.

21. Zheng, Y., Wang, J., Zhu, Y. & Wang, A. (2015) Research and application of kapok fiber as an absorbing material: A mini review. *Journal of Environmental Sciences (China)*, **27**, 21–32.

22. Abdullah, R., Astira, D., Zulfiani, U., Widyanto, A. R., Hidayat, A. R. P., Sulistiono, D. O., Rahmawati, Z., Gunawan, T., Kusumawati, Y., Othman, M. H. D. & Fansuri, H. (2024) Fabrication of composite membrane with microcrystalline cellulose from lignocellulosic biomass as filler on cellulose acetate based membrane for water containing methylene blue treatment. *Bioresource Technology Reports*, **25**, 101728.

23. Sazman, N. S. N., Ahmad Rafaie, H., Daud, S., Mohd Shohaimi, N. A., Abu Bakar, M. A. A. and Mohd Hir, Z. A. (2023) Extraction and physicochemical characterization of microcrystalline cellulose from Gigantochloa scortechinii. *Malaysian Journal Chemistry*, **25(3)**, 323–330.

24. Tarchoun, A. F., Trache, D. & Klapötke, T. M. (2019) Microcrystalline cellulose from Posidonia oceanica brown algae: Extraction and characterization. *International Journal of Biological Macromolecules*, **138**, 837–845.

25. Borsoi, C., Ornaghi, H. L., Scienza, L. C., Zattera, A. J. & Ferreira Carlos, A. (2017) Isolation and characterisation of cellulose nanowhiskers from microcrystalline cellulose using mechanical processing. *Polymers and Polymer Composites*, **25**, 563–570.

26. Sartika, D., Syamsu, K., Warsiki, E. & Fahma, F. (2020) Isolation of microfiber cellulose from kapok fiber (Ceiba pentandra) by using chemical-hydrothermal treatment. *Ecology, Environment and Conservation*, **26**, 654–662.